2007

Coherent multiple scattering effect in DIS

Jun Li
Iowa State University

Coherent multiple scattering effect in DIS

by

Jun Li

A thesis submitted to the graduate faculty

in partial fulfillment of the requirements for the degree of

MASTER OF SCIENCE

Major: Nuclear Physics

Program of Study Committee:
Xiaofeng Guo, Co-major Professor
James P. Vary, Co-major Professor
Kerry Whisnant
James W. Evans

Iowa State University

Ames, Iowa

2007

UMI Number: 1443134

UMI

UMI Microform 1443134

ProQuest Information and Learning Company
300 North Zeeb Road
P.O. Box 1346
Ann Arbor, MI 48106-1346

DEDICATION

To my wife

TABLE OF CONTENTS

LIST OF FIGURES

ACKNOWLEDGMENTS

I would like to take this opportunity to express my thanks to my advisor, Professor Xiaofeng Guo, for her guidance, patience and support throughout this research. Her encouragement have often inspired me and her questions and observations have provided valuable guidance for this research.

I also thank all my committee members for their efforts and contributions to this work.

Sincere thanks extend to Professors Jianwei Qiu and James P. Vary who have taught me so many things about not only the fundamentals but also the new progress on the nuclear physics.

Finally I want to thank graduate students Zhongbo Kang, Oleg Antipin and Postdoctoral Research Associate Piyabut Burikham for the discussion about physics in private or our regular group meetings.

This work was supported in part by the U.S.National Science Foundation under Grant No.0340729.

ABSTRACT

In nuclear medium, the parton can lose its energy by gluon radiation and collisional energy loss. In order to understand heavy quark energy loss, the collisional energy loss could be an important source for the observed suppression of hadron production.

We calculate the multiple scattering effect on single hadron production in semi-inclusive lepton-nucleus deeply inelastic scattering. We show that the quantum interference of multiple scattering amplitudes leads to suppression in hadron productions. At the leading power in medium length, the suppression can be approximately expressed in terms of a shift in z_h of the fragmentation function, and could be therefore interpreted as the collisional energy loss. We compare our calculation with existing experimental data. Our approach can be extended to other observables in hadronic collisions.

CHAPTER 1. INTRODUCTION

The Relativistic Heavy Ion Collider (RHIC) at Brookhaven National Laboratory has produced a new state quark-gluon plasma (QGP) in Au-Au collisions. In order to know its formation and physical properties, one can use the probes which can tentatively investigate its properties. One of these good probes is the jet quenching. A jet is an energetic beam of ordinary particles produced when a pair of partons are knocked out of a proton during a collision between two nuclei. Due to the conservation of momentum, after the hard collision, one parton moves away from the QGP and the other one moves toward the QGP. When the parton is propagating through the hot QGP after the initial hard collision, it will interact with the medium, losing the significant energy. Finally there is the strong suppression of high transverse momentum hadron observed in relativistic heavy ion collisions compared with hadron production in proton-proton collisions. This is considered to be an evidence for the existence of QGP (1).

At RHIC, in Au-Au collisions, there is large energy involved (the gold nuclei can be accelerated up to 100 GeV/c per nucleon). During the collision, there is the large momentum transfer which guarantees perturbative QCD (pQCD) calculations can provide a solid theoretical framework. The factorization assumes that the hard partonic subprocess can be separated from the long distance, non-perturbative physics such as the parton distribution function and the parton fragmentation function. The hard part can be calculated by use of pQCD. Both the parton distribution function and fragmentation function are process independent and can be measured from the experiment even though they can not be calculated perturbatively. Thus the total cross section can be expressed in terms of the convolution between the parton distribution function, fragmentation function and hard partonic cross section.

In the hot QGP, a parton loses energy through two different ways. One is collisional energy loss. Parton loses energy by exchanging energy and momentum with the collision centers in the QGP. And the other one is media-induced gluon radiation. The radiated gluon carries out the energy of the fast moving parton (2). From these two ways, a parton can either transfer some of its energy to the surrounding medium or lose its energy by radiating the gluons.

Heavy quarks can also be good probes of the hot QGP. In the QGP, the deconfined quarks and gluons will modify the interaction between the heavy quark and antiquark. Then the potential between heavy quark and antiquark can be screened at high temperature. Therefore the suppression of heavy quark bound states can be the signature of the existence of QGP. Except that heavy quark can serve as the probes of the screening effect, it can also be used as the probe for the color charge density in the medium through the energy loss. However, heavy quark energy loss is different from that of the light quark and gluon. At leading order in the QCD coupling constant, the heavy quark can only interact with gluons in the medium. Also gluon radiation from a heavy quark with mass M and energy E is strongly suppressed at forward angle $\theta < \theta_0 = M/E$. Therefore we expect that heavy quarks will lose much less energy than light quarks if the radiative energy loss is the only source of the suppression (3). But recent data indicate that heavy quarks would lose the same amount of energy as that of the light quarks(4). This tells that heavy quark energy loss is different from the light quarks for which the radiative energy loss is dominant. And we will show in this thesis that there is another source, coherent multiple scattering effect, which can consequently lead to the suppression of hadron production rate.

In addition to understanding how the QGP as the hot medium affects the hadron production, we also need to understand cold nuclear effects on the hadron production.

The observed nuclear dependence can be classified into three categories (5). The first one is the initial-state interaction between the parton and nucleus inside the nucleus. The second one is the initial parton-nucleus interaction. The last one is the final-state parton-nucleus interaction.

The initial-state interaction inside the nucleus will change the twist 2 parton distribution function. As a result, the nuclear parton distribution function will be different from the simple sum of the total nucleon's parton distribution. This is the "EMC" effect (6). The initial parton-nucleus interaction and final state parton-nucleus interaction will involve at least two partons during the hard collisions. It will cause the "Cronin effect" and A^{α}-dependence with $\alpha > 1$ (7).

We can distinguish two kinds of the final state interactions between the parton and nucleus. After the hard collision, at the high values of the energy-squared scale, one can show that the long-distance part can be factorized out from the short-distance part using the factorization theorem. When the highly off-shell scale parton is propagating in the nuclear medium, it will interact with the nuclear medium such that there is medium-induced gluon radiation. Since this kind of parton-nucleus interaction happens after we factorize the long-distance part from the short-distance part, it will modify the Dokshitzer-Gribov-Lipatov-Altarelli-Parisi (DGLAP) equations which is the conventional QCD evolution function and the result demonstrates the nuclear modification of the quark fragmentation functions (8).

On the other hand, the multiple scattering between the parton and the nuclear medium can happen coherently following the first hard scattering, before there is soft collinear gluon radiation. As we will see in Chapter 3, this kind of coherent multiple scattering will consequently shift the z_h-dependence of the quark fragmentation function. As a result, it will demonstrate the modification of the final hadron production such that consequently there is strong suppression of the hadron production rate, which might be interpreted as the collisional energy loss (9).

This thesis is organized as follows. In Chapter 2, the general formula for the cross section of semi-inclusive Deep Inelastic Scattering (DIS) are given in terms of the parton distribution functions, the parton fragmentation functions and partonic cross sections. The conventional factorization method used to separate the long-distance part out from the short-distance part is also discussed. In Chapter 3, the coherent multiple scattering between the parton and medium is discussed. Taking advantage of the factorization theorem, we calculate the double multiple scattering effect at first. Then we generalize our result to n-additional scattering. After summing over all order contributions, we found that the effect of coherent multiple scattering of the propagating quark is equivalent to a shift of z_h in the fragmentation function. In Chapter 4, we use our result to calculate the multiplicity ratio R_M which represents the number of hadrons produced for a nuclear target to that for a deuterium target. Our result shows that there is the suppression of hadron production for the nuclear target compared with the deuterium target, which is consistent with experimental data. The summary and conclusions of this thesis are presented in Chapter 5.

CHAPTER 2. SEMI-INCLUSIVE DEEP INELASTIC SCATTERING

In analogy with Rutherford's interference from α-particle scattering that the atom contained a nucleus, one can use high energy electrons to probe the substructure of the proton. At the leading order, the electron interacts with the proton by exchanging a virtual photon with momentum transfer Q^2. From the uncertainty principle in quantum mechanics, the virtual photon can resolve the space-time distances of proton as small as $1/\sqrt{Q^2}$. If the proton contains free partons with some distribution of the momentum and energy, the virtual photon has a significant probability to scatter from the parton such that this distribution can be measured. The measurement of inelastic electron-proton scattering demonstrated that the parton distribution of momentum and energy has the Bjorken scale invariance, which says that in the free parton model the parton distribution function is independent of momentum transfer Q^2. However in real Quantum Chromodynamics (QCD), the parton distribution function does depend on the momentum transfer Q^2. The dependence of the parton distribution function in Q^2 is described by DGLAP equations (10). These equations tell how the parton distribution function evolves with Q^2. In QCD, if we define x as the fraction of proton momentum carried by the parton, the partons tend to split into multiple partons with smaller x. So if Q^2 increases, the virtual photon will see more partons with smaller momentum fraction x. As a result, the parton distribution function increases in the small x region as Q^2 increases.

Free quarks can not exist. After the hard collision, the parton will become the hadrons which can be observed by the experiment. We can use the fragmentation function to describe the probability to produce a hadron with the fraction z_h of the virtual photon momentum. In real QCD, the fragmentation function also depends on the momentum transfer Q^2 and its evolution can be described by the DGLAP equations.

2.1 Semi-inclusive DIS Cross Section

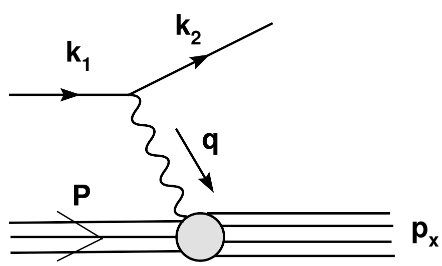

Figure 2.1 Deep inelastic scattering.

We consider the scattering of a high-energy electron off a proton target. From Fig. 2.1, we can see that the incoming proton has momentum P. The initial and final momenta of the electron are k_1 and k_2. In the leading order and without considering the weak interaction, the electron interacts with the proton by exchanging a virtual photon. From the energy-momentum conservation, the virtual photon carries the four-dimensional momentum $q = k_2 - k_1$. Since this is the t-channel interaction between the electron and proton, the vector q is spacelike. So we can define another variable Q^2 which satisfies the relation $q^2 = -Q^2$.

The cross section for DIS can be written in general as

$$d\sigma = \frac{1}{2s} \left| \bar{M}_{k_1 p \to k_2 X} \right|^2 d(PS), \tag{2.1}$$

where $s = (P + k_1)^2$ is the total invariant mass of the lepton-nucleon system. $\left|\bar{M}\right|^2$ is the square of the matrix element, averaged over the initial spin and summed over final spins. And $d(PS)$ is the phase space. For the process $1+2 \to 3+4$,

$$d(PS) = \frac{d^3p_3}{(2\pi)^3 2E_3} \frac{d^3p_4}{(2\pi)^3 2E_4} (2\pi)^4 \delta^4(p_1+p_2-p_3-p_4). \quad (2.2)$$

The square of the matrix element can be written as the product of the leptonic tensor $L^{\mu\nu}$ and the hadronic tensor $W_{\mu\nu}$.

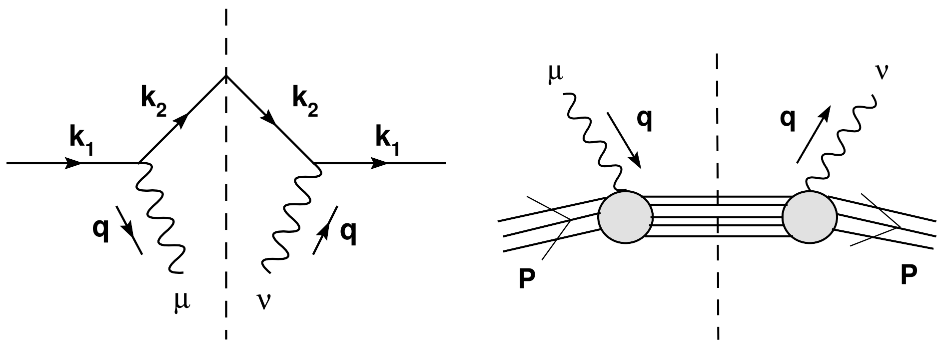

Figure 2.2 Left: Leptonic tensor $L^{\mu\nu}$; Right: Hadronic tensor $W_{\mu\nu}$.

From the Fig. 2.2, the leptonic tensor

$$L^{\mu\nu}(k_1,k_2) = \mathrm{Tr}(\gamma\cdot k_1 \gamma^\mu \gamma\cdot k_2 \gamma^\nu)/2. \quad (2.3)$$

The hadronic tensor contains all the information about the interaction of the electromagnetic current J_μ with the target proton P. In general, we have

$$\begin{aligned} W_{\mu\nu} &= \frac{1}{4\pi}\sum_X \langle P|J_\mu^+|X\rangle\langle X|J_\nu|P\rangle\,(2\pi)^4\,\delta^4(q+P-P_X) \\ &= \frac{1}{4\pi}\int d^4z\, e^{iq\cdot z}\langle P|J_\mu^+(z)\,J_\nu(0)|P\rangle \\ &= \frac{1}{4\pi}\int d^4z\, e^{iq\cdot z}\langle P|[J_\mu^+(z), J_\nu(0)]|P\rangle. \end{aligned} \quad (2.4)$$

From the gauge invariance, we know the hadronic tensor $W_{\mu\nu}$ satisfies the relationship

$$q^\mu W_{\mu\nu} = q^\nu W_{\mu\nu} = 0. \quad (2.5)$$

Then in general, the $W_{\mu\nu}$ can be expressed in terms of the structure functions F_1 and F_2,

$$W_{\mu\nu}(P,q) = (-g_{\mu\nu} + \frac{q_\mu q_\nu}{q^2})F_1 + \frac{1}{P\cdot q}(P_\mu - \frac{P\cdot q}{q^2}q_\mu)(P_\nu - \frac{P\cdot q}{q^2}q_\nu)F_2 \quad (2.6)$$

We can check that Eqn.(2.6) satisfies the gauge invariant constraint Eqn.(2.5).

We consider the production of a single hadron of momentum p_h in DIS. The semi-inclusive DIS cross section can be written as

$$\frac{d\sigma_{eP\to ehX}}{dx_B dQ^2 dz_h} = \frac{1}{8\pi}\,\frac{e^4}{x_B^2 s^2 Q^2}\,L^{\mu\nu}(k_1,k_2)\,\frac{dW_{\mu\nu}}{dz_h}\ , \tag{2.7}$$

where $z_h \equiv P\cdot p_h/P\cdot q = 2x_B P\cdot p_h/Q^2$ is the fraction of the photon momentum carried by the observed hadron. The Bjorken variable $x_B = Q^2/(2P\cdot q)$ with $Q^2 = -q^2$. The leptonic tensor $L^{\mu\nu}(k_1,k_2)$ is given by Eqn.(2.3).

The hadronic tensor $W_{\mu\nu}$ contains the strong interaction contribution, which is very different from that of Quantum Electrodynamics (QED). The coupling constant for QCD is very large at low energy scales, such that hadronic tensor contains the non-perturbative part which makes the calculation much more complicated than QED.

In the next section, we will show that due to the asymptotic freedom of QCD, we can use the factorization theorem to separate the non-perturbative part out of the short-distance part which can be calculated perturbatively.

2.2 Asymptotic Freedom and Factorization

QCD is an asymptotically free theory. The coupling $\alpha_s(Q^2)$ becomes smaller as the momentum transfer Q^2 increases. In DIS, the virtual photon carries large Q^2. For hard scattering, the coupling constant is small. Thus we should be able to calculate this hard scattering part using pQCD.

This can also be understood from the Parton-model.

If the virtual photon carries large momentum Q^2, the hard-scattering can resolve states whose lifetimes are as short as $1/\sqrt{Q^2}$. As long as the momentum transfer Q^2 is large enough, the hard scattering time t_{hard} is much smaller than the parton interacting time within the hadron t_{hadron}. In the leading power, the interaction among partons is negligible. The photon interacts with one parton which carries the fraction of the proton incoming momentum with some probability. Therefore the scattering amplitudes where hadrons are scattered with large momentum transfer can often be expressed as a convolution of the parton distribution function and the hard-scattering quark-photon subprocess scattering amplitude.

The free quark can not exist because of confinement. After the hard scattering, the scattered parton can not be free to propagate over macroscopic distances and has to be confined inside hadrons. This is due to long-distance physics and can not be calculated perturbatively. Just like for the parton distribution functions, the interference between the parton hadronization process and the hard part can be neglected such that we can use the factorization to separate it out. Then the effect of the non-perturbative hadronization process is expressed in terms of a universal fragmentation function.

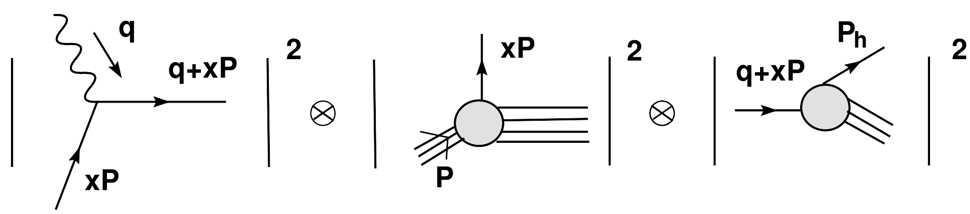

Figure 2.3 The hadronic tensor can be factorized in terms of the convolution between hard part, the parton distribution function and the parton fragmentation function.

From the discussion above, we can sketch the whole process of semi-inclusive DIS in Fig.2.3. From this figure, we can see that the cross section of semi-inclusive DIS can be written as

$$\sigma(Q^2) = H \otimes \psi_q \otimes D_{q\to h}, \tag{2.8}$$

where ψ_q is the parton distribution function, $D_{q\to h}$ is the parton fragmentation function, H represents underlying partonic subprocess and $\otimes$ represents the convolution. Both the parton distribution function and the fragmentation function represent the non-perturbative long distance part which are universal and can be measured experimentally. The underlying quark-gluon subprocess is the short-distance hard part and can be calculated perturbatively.

So far we have given a qualitative argument why the physical observables such as the cross section can be written in terms of the convolution between the short distance part and long distance part. In the rest part of this section, we will use the factorization theorem to achieve this goal.

Before we do the calculation, we choose the light-cone coordinates

$$\begin{aligned} \bar{n}^\mu &= (1, 0, 0^\perp), \\ n^\mu &= (0, 1, 0^\perp). \end{aligned} \tag{2.9}$$

In terms of the light cone coordinates, the incoming momentum of the proton P and the momentum of the virtual photon q can be decomposed as

$$\begin{aligned} P^\mu &= P^+ \bar{n}^\mu, \\ q^\mu &= -x_B P^+ \bar{n}^\mu + \frac{Q^2}{2 x_B P^+} n^\mu. \end{aligned} \tag{2.10}$$

Also through this thesis, we fix the gauge by choosing $n \cdot A = 0$.

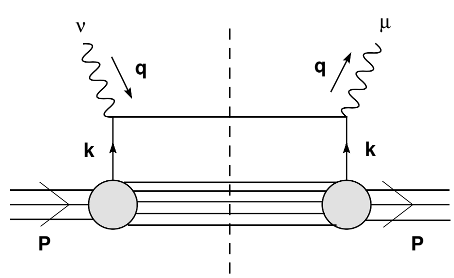

Figure 2.4 The lowest order hadronic tensor.

At first from Fig.2.4, we can see that the lowest order hadronic tensor $W^{(0)}_{\mu\nu}$ can be written as

$$W^{(0)}_{\mu\nu} = \int \frac{d^4 k}{(2\pi)^4} \, \mathrm{Tr}[\hat{T}(P,k) \, \hat{H}^{(0)}_{\mu\nu}(k,q)], \tag{2.11}$$

where $\hat{H}^{(0)}_{\mu\nu}$ represents hard scattering part between the photon and the parton with momentum k. And the long-distance part $\hat{T}(P,k)$ which represents the probability to find a parton carrying the momentum k can be expressed using the wavefunction

$$\hat{T}(p,k) = \int d^4y\, e^{ik\cdot y}\langle P|\bar{\psi}(0)\psi(y)|P\rangle. \tag{2.12}$$

In the light-cone coordinates, the incoming proton has very large momentum along the $\bar{n}$ direction. With the negligible transverse momenta, all the constituents inside the proton are moving parallel to this direction with fraction momentum xP. After we use this approximation, the short-distance part $\hat{H}^{(0)}_{\mu\nu}$ can be approximated as

$$\hat{H}^{(0)}_{\mu\nu}(k,q) \simeq \hat{H}^{(0)}_{\mu\nu}(xP,q), \tag{2.13}$$

where x is the fraction of the incoming hadron momentum carried by the parton. Then Eqn.(2.11) will be written as

$$W^{(0)}_{\mu\nu} = \int dx\, \mathrm{Tr}[\hat{T}(x)\, \hat{H}^{(0)}_{\mu\nu}(xP,q)], \tag{2.14}$$

where $\hat{T}(x)$ is expressed as

$$\begin{aligned}\hat{T}(x) &= \int \frac{d^4k}{(2\pi)^4}\delta(x-\frac{k^+}{P^+})\hat{T}(P,k) \\ &= \int \frac{P^+dy^-}{2\pi}e^{ixP^+y^-}\langle P|\bar{\psi}(0)\psi(y)|P\rangle. \end{aligned}\tag{2.15}$$

In order to get Eqn.(2.14), we insert 1 under the integral of Eqn.(2.11) in the following form:

$$1 = \int dx\delta(x-\frac{k^+}{P^+}). \tag{2.16}$$

Note that Eqn.(2.14) contains the trace calculation which couples the hard part with the long distance part. We can separate the trace. Then Eqn.(2.14) can be written as

$$W^{(0)}_{\mu\nu} = \int dx\, T_\alpha(x)\, \mathrm{Tr}[\frac{1}{2}\,\gamma^\alpha\, \hat{H}^{(0)}_{\mu\nu}(xP,q)]. \tag{2.17}$$

Also note that in Eqn.(2.17), we need to sum over the repeated Lorentz index α. In order to decouple the long distance part and the short distance part, we can separate the Lorentz index α (11). After we do this, then Eqn.(2.17) can be written as

$$W_{\mu\nu}^{(0)} = \sum_q \int dx\, \psi_q(x)\, \mathrm{Tr}[\frac{1}{2}\gamma \cdot P\, \hat{H}_{\mu\nu}^{(0)}(xP, q)], \tag{2.18}$$

where the quark distribution function $\psi_q(x)$ with flavor q is defined as

$$\psi_q(x) = \int \frac{dy^-}{2\pi} e^{ixP^+y^-} \langle P|\bar{\psi}(0)\frac{\gamma^+}{2}\psi(y^-)|P\rangle. \tag{2.19}$$

By use of the factorization, Eqn.(2.18) shows that the lowest order hadronic tensor $W_{\mu\nu}^{(0)}$ can be written in terms of the convolution between the short-distance part $\hat{H}_{\mu\nu}^{(0)}$ and parton distribution function $\psi_q(x)$. The result obtained from the factorization is consistent with the Parton-model.

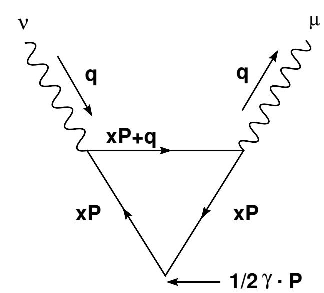

Figure 2.5 The hard part from the factorization

For the lowest order, the Feynman diagram for short-distance part $\hat{H}_{\mu\nu}^{(0)}$ is sketched in Fig.2.5. Note that using the factorization, there is a cut vertex $\frac{1}{2}\gamma \cdot P$ multiplied with $\hat{H}_{\mu\nu}^{(0)}$. Then we can evaluate this perturbative part using the Feynman rule from QCD. Therefore we obtain

$$\begin{aligned} & \mathrm{Tr}[\frac{1}{2}\gamma \cdot P\hat{H}_{\mu\nu}^{(0)}(xP, q)] \\ = \; & \frac{e_q^2}{4\pi}\, \mathrm{Tr}[\frac{1}{2}\gamma \cdot P\, \gamma_\mu\, \gamma \cdot (xP + q)\, \gamma_\nu]\, 2\pi\delta((xP + q)^2) \\ = \; & e_q^2\, \frac{\delta(x - x_B)}{2P \cdot q}[P_\mu(xP + q)_\nu + (xP + q)_\mu P_\nu - (P \cdot q)\, g_{\mu\nu}], \end{aligned} \tag{2.20}$$

where e_q is the electric charge of quark with flavor q.

From Eqn.(2.20), we can show that hadronic tensor $W^{(0)}_{\mu\nu}$ satisfies the gauge invariance constraint

$$q^\mu W^{(0)}_{\mu\nu} = q^\nu W^{(0)}_{\mu\nu} = 0. \tag{2.21}$$

The structure function $F_1(x_B,Q^2)$ and $F_2(x_B,Q^2)$ then can be extracted from the lowest order partonic tensor

$$\begin{aligned} F_1(x_B,Q^2) &= \frac{1}{2}\sum_q \int dx \psi_q(x)[e_q^2\delta(x-x_B)] \\ &= \frac{1}{2}\sum_q e_q^2\psi_q(x_B), \\ F_2(x_B,Q^2) &= \sum_q e_q^2 x_B \psi_q(x_B). \end{aligned} \tag{2.22}$$

From the expression of $F_1(x_B,Q^2)$ and $F_2(x_B,Q^2)$, we obtain the famous Callan-Gross relation $F_2 = 2x_B F_1$.

We have seen how to get the lowest order hadonic tensor by using factorization. The results show that the hadronic tensor can be expressed as the convolution between the hard part scattering and parton distribution function. However there is no discussion made of the nature of the final hadronic state.

We can consider the production of detected hadrons in the current fragmentation region (not the proton target fragmentation region). Different from the inclusive scattering process, there is an extra kinematic degree of freedom associated with the detected hadron momentum P_h. Since the hadron is detected in the current fragmentation region, P_h emerges along the direction of q. Then we can define the parton fragmentation function $D_{q\to h}(z_h,Q^2)$ which represents the probability of the parton q to produce the hadron h carrying the fraction of photon momentum z_h.

We can assume that the fragmentation process is independent of the hard scattering process. Using the factorization theorem, we will see that the semi-inclusive cross section can be expressed as the convolution of the hard scattering part, the parton distribution function and the fragmentation function.

We consider the lowest order contribution to single hadron DIS cross section.

After we factorize the parton distribution function out, the hadronic tensor is

$$W^{(0)}_{\mu\nu} \simeq \sum_q \int dx\, \psi_q(x, Q^2)\, \hat{W}^{(0)}_{\mu\nu}(xP, q, P_h) \tag{2.23}$$

For semi-inclusive DIS, the $\hat{W}^{(0)}_{\mu\nu}$ contains the parton fragmentation function associated with the detected hadron. We are going to show that using factorization, we can separate it out,

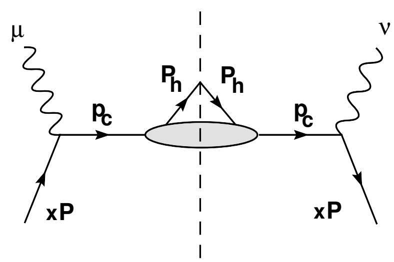

Figure 2.6 the semi-inclusive hadronic tensor

At first, from Fig. 2.6, we have

$$\hat{W}^{(0)}_{\mu\nu}(xP, q, P_h) \simeq \int dz_h \mathrm{Tr}[\frac{1}{2}\gamma \cdot P \hat{H}^{(0)}_{\mu\nu}(xP, q, \frac{P_h}{z_h})\hat{T}(z_h, P_h)](2\pi)^4\delta^4(p_c - q - k)\frac{d^3P_h}{(2\pi)^3 2E_h} \tag{2.24}$$

In order to get Eqn.(2.24), we have used the collinear approximation $P_h \simeq z_h\, p_c$. And we also insert 1 under the integral of Eqn.(2.24) in the form:

$$1 = \int dz_h\, \delta(z_h - \frac{P_h \cdot \bar{n}}{p_c \cdot \bar{n}}). \tag{2.25}$$

The long-distance part $\hat{T}(z_h, P_h)$ satisfies the equation

$$\begin{aligned} \hat{T}(z_h, P_h) &= \int \frac{d^4p_c}{(2\pi)^4}\delta(z_h - \frac{P_h \cdot \bar{n}}{p_c \cdot \bar{n}}) \sum_X \langle 0|\Psi(0)|P_h X\rangle\langle P_h X|\bar{\Psi}(0)|0\rangle \\ & \quad (2\pi)^4\delta^4(p_c - P_h - \sum_X P_X) \prod_X \frac{d^3P_X}{(2\pi)^3 2E_X} \\ &= \int \frac{d^4p_c}{(2\pi)^4}\delta(z_h - \frac{P_h \cdot \bar{n}}{p_c \cdot \bar{n}}) \int d^4y e^{ip_c\cdot y}\, \langle 0|\Psi(y)|P_h\rangle\langle P_h|\bar{\Psi}(0)|0\rangle \end{aligned} \tag{2.26}$$

In order to simplify Eqn.(2.26), we can choose the light-cone variable

$$\frac{d^4 p_c}{(2\pi)^4} \rightarrow \frac{dp_c^+ \, dp_c^- \, dp_c^\perp}{(2\pi)^4},$$
$$d^4 y \rightarrow d\,y^+ \, d\,y^- \, d\,y^\perp. \tag{2.27}$$

After we integrate the dp_c^+, dp_c^-, $dp_c^\perp$ and dy^-, $dy^\perp$, Eqn.(2.26) will be

$$\hat{T}(z_h, P_h) = \frac{P_h^-}{z_h^2} \int \frac{dy^+}{2\pi} \, e^{iP_h^- \, y^+/z_h} \, \langle 0|\Psi(y^+)|P_h\rangle \, \langle P_h|\bar{\Psi}(0)|0\rangle, \tag{2.28}$$

As we have seen, in Eqn.(2.24) there is the trace calculation which couples the short-distance part with the long-distance part. We can use the same strategy as we have done for the inclusive cross section to decouple them. Therefore, we obtain

$$E_h \frac{dW_{\mu\nu}^{(0)}}{d^3 P_h} = \sum_q \int dx \, \psi_q(x) \int \frac{dz}{z_h^2} D_{q\rightarrow h}(z_h) \tilde{W}_{\mu\nu}^{(0)}(xP, q, \frac{P_h}{z_h}), \tag{2.29}$$

where $\tilde{W}_{\mu\nu}^{(0)}$ is written as

$$\tilde{W}_{\mu\nu}^{(0)} = \frac{1}{2(2\pi)^3} \mathrm{Tr}[\frac{1}{2}\gamma \cdot P \hat{H}_{\mu\nu}^{(0)}(xP, q, \frac{P_h}{z_h})\gamma \cdot \frac{P_h}{z_h}](2\pi)^4 \delta^4(\frac{P_h}{z_h} - q - k), \tag{2.30}$$

Then we can define the fragmentation function $D_{q\rightarrow h}$ which is

$$D_{q\rightarrow h}(z_h) \;=\; z_h \int \frac{dy^+}{2\pi} e^{ip_c^- y^+} \frac{1}{4} \mathrm{Tr}[\gamma \cdot \bar{n} \, \left\langle 0 \left| \Psi(y^+) \right| P_h \right\rangle \left\langle P_h \left| \bar{\Psi}(0) \right| 0 \right\rangle] \tag{2.31}$$

For the lowest order, the hard part $\tilde{W}_{\mu\nu}^{(0)}$ is given by

$$\tilde{W}_{\mu\nu}^{(0)} = \frac{1}{8\pi} \mathrm{Tr}[\frac{1}{2}\gamma \cdot P \gamma_\mu \gamma \cdot (\frac{P_h}{z_h})\gamma_\nu] \, e_q^2 \, (2\pi)\delta^4(xP + q - \frac{P_h}{z_h}), \tag{2.32}$$

where we have used the relation $k = xP$.

Plugging Eqn.(2.32) into Eqn.(2.29), we obtain the lowest order hadronic tensor $W_{\mu\nu}^{(0)}$ which is written as the convolution between the parton distribution function, the fragmentation function and the hard part,

$$E_h \frac{dW_{\mu\nu}^{(0)}}{d^3 P_h} \;=\; \frac{1}{2} \sum_q \int dx \psi_q(x) \int \frac{dz_h}{z_h^2} D_{q\rightarrow h}(z_h) [P_\mu (xP + q)_\nu + P_\nu (xP + q)_\nu - (P \cdot q) \, g_{\mu\nu}]$$
$$\delta^4(xP + q - \frac{P_h}{z_h}), \tag{2.33}$$

In Eqn.(2.33), we can integrate d^3P_h out by taking advantage of the relationship

$$\frac{d^3P_h}{E_h} = d^4P_h\,\delta(P_h^2). \tag{2.34}$$

Then we can get the lowest order hadronic tensor $W_{\mu\nu}^{(0)}$ which is

$$\frac{dW_{\mu\nu}^{(0)}}{dz_h} = \frac{1}{2}\,e_{\mu\nu}^T \sum_q \psi_q(x_B, Q^2)\, D_{q\to h}(z_h, Q^2), \tag{2.35}$$

where $e_{\mu\nu}^T$ is defined as

$$e_{\mu\nu}^T = \frac{1}{P\cdot q}\,[P_\mu q_\nu + q_\mu P_\nu] + \frac{2x_B}{P\cdot q}\,P_\mu P_\nu - g_{\mu\nu}. \tag{2.36}$$

As we have seen that using the factorization theorem , the semi-inclusive DIS cross section can be written as the convolution between hard scattering part, the parton distribution function and the fragmentation function. The results give the clear physical picture: Since the virtual photon has large momentum, it will interact with one parton very quickly as if all the interaction between the partons is frozen. The interaction probability between the virtual photon and the parton with fraction momentum x will be proportional to the parton distribution function. After the scattering, in the current fragmentation region, the detected hadrons are produced with a probability which is proportional to the parton fragmentation function.

CHAPTER 3. COLD NUCLEAR EFFECT IN DIS

When a fast moving parton is propagating in the medium, it can lose its energy and momentum by interacting with the medium. Understanding the basic feature of this high-energy nuclear process is important in ultra-relativistic heavy ion collisions, in high-energy proton-nucleus reactions and in high-energy lepton-nucleus interactions. The energetic parton can lose its energy and momentum through collisional energy loss and gluon radiation. For light quarks and gluons, the latter is thought to be dominant. However as we have mentioned in Chapter 1, the radiative energy loss of a heavy quark should be less than that of the light quarks due to the mass effect of heavy quark. Therefore to understand the recent data that a heavy quark loses the same amount of energy as a light quark, we need to find a new source which leads to suppression of hadron production.

Here we present a new source of suppression from coherent multiple scattering. In this treatment, quantum interference between the different scattering process is taken into account.

In order to understand the coherent multiple scattering, at first we need to distinguish two kinds of final state interaction between the struck parton and nuclear matter.

The first kind of final state interaction is given by the left plot in Fig.3.1. After the first hard scattering, the interaction between the struck parton and nucleus will lead to the media-induced gluon radiation. If the radiated gluon is collinear to the final state hadron, there is the infrared divergence which is labeled by crosses "$\times$". This divergence belongs to the long distance physics and can not be calculated perturbatively. A good way to solve this problem is to use the factorization to separate this long distance part out. Then the effect the multiple scattering leads to the modification to the quark fragmentation functions.

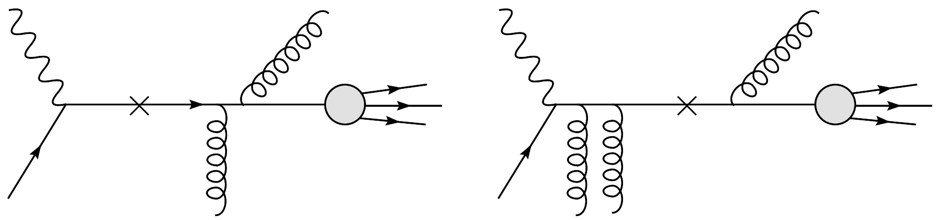

Figure 3.1 Final state interaction between struck quark and nucleus. Left: Final state interaction modifies the fragmentation function; Right: Coherent multiple scattering between the struck quark and nucleus suppresses the hadron production rate.

The second kind of final state interaction is given by the right plot in Fig.3.1. After the first hard scattering between the parton and the virtual photon, the struck parton would coherently interact with the nuclear medium before it radiates the collinear gluon.

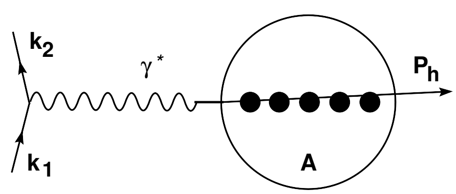

Figure 3.2 The process shows how the struck quark with small P_T interacts coherently with the nucleus.

This process is also sketched in Fig.3.2. Due to the large size of nucleus, the struck parton propagates in the nucleus and rescatters coherently with the remnant of the nucleus at the same impact parameter. Since this kind multiple scattering is associated with the first hard scattering, by use of the factorization theorem, the contribution from the multiple scattering can be factorized as the convolution between short-distance hard part and long-distance non-perturbative part. The long-distance part represents the multiparton correlation function in nuclei (12). Just like the parton distribution function, this multiparton correlation function is nonperturbative and can be measured experimentally.

In the next several sections, we will find that this kind of coherent multiple scattering can modify the hadron production rate. And it can be another source for the suppression of hadron production.

3.1 Double Scattering Contribution

In this section, we consider semi-inclusive DIS cross section with double scattering. The process is sketched in Fig.3.3.

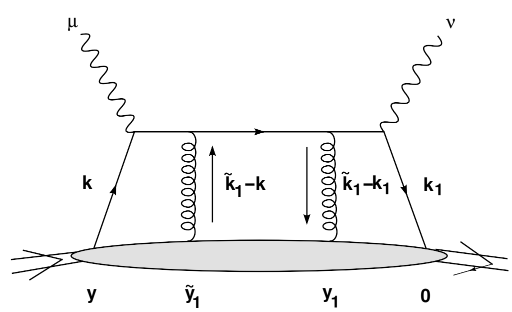

Figure 3.3 Double scattering Feynman diagram for the semi-inclusive hadronic tensor without the nonperturbative parton-to-hadron fragmentation function attached.

The hadronic tensor with double scattering is given by

$$\begin{aligned} W^{(1)}_{\mu\nu} &= \frac{1}{4\pi}\int \frac{d^4k}{(2\pi)^4}\frac{d^4k_1}{(2\pi)^4}\frac{d^4\tilde{k}_1}{(2\pi)^4}\mathrm{Tr}[\hat{H}^{\alpha\beta}_{\mu\nu}(k,k_1,\tilde{k}_1,q)\hat{T}^{(1)}_{\alpha\beta}(k,k_1,\tilde{k}_1)] \\ &\simeq \frac{1}{4\pi}\int dx d\tilde{x}_1 dx_1 \frac{d^4k}{(2\pi)^4}\frac{d^4k_1}{(2\pi)^4}\frac{d^4\tilde{k}_1}{(2\pi)^4}\delta(x-\frac{k\cdot n}{p\cdot n})\delta(x_1-\frac{k_1\cdot n}{p\cdot n})\delta(\tilde{x}_1-\frac{\tilde{k}_1\cdot n}{p\cdot n}) \\ &\quad \mathrm{Tr}[\hat{H}^{\alpha\beta}_{\mu\nu}(x,\tilde{x}_1,x_1,q)\hat{T}^{(1)}_{\alpha\beta}(k,k_1,\tilde{k}_1)] \end{aligned} \tag{3.1}$$

The second line of Eqn.(3.1) is obtained when we take the approximation that all the quarks and gluons move with the same direction as the nucleus. And $x, \tilde{x}_1$ and x_1

represent the fraction of the nuclear momentum. Under the integral of Eqn.(3.1), we have inserted the identity

$$1 = \int dx d\tilde{x}_1 dx_1 \delta(x - \frac{k \cdot n}{p \cdot n})\delta(\tilde{x}_1 - \frac{\tilde{k}_1 \cdot n}{p \cdot n})\delta(x_1 - \frac{k_1 \cdot n}{p \cdot n}) \tag{3.2}$$

We can use the same strategy used in Chapter 2 to separate the trace calculation. After we do this, the hadronic tensor will be written as

$$W^{(1)}_{\mu\nu} = \int dx d\tilde{x}_1 dx_1 H^{\alpha\beta}_{\mu\nu}(x, \tilde{x}_1, x_1, q) T^{(1)}_{\alpha\beta}(x, \tilde{x}_1, x_1), \tag{3.3}$$

where $T^{(1)}_{\alpha\beta}(x, \tilde{x}_1, x_1)$ contains the multiple parton correlation function and is written as

$$\begin{aligned} T^{(1)}_{\alpha\beta}(x, \tilde{x}_1, x_1) &= \mathrm{Tr}[\hat{T}^{(1)}_{\alpha\beta}(x, \tilde{x}_1, x_1)\gamma \cdot n]\frac{1}{2p \cdot n} \\ &= \int \frac{d^4k}{(2\pi)^4}\frac{d^4k_1}{(2\pi)^4}\frac{d^4\tilde{k}_1}{(2\pi)^4}\delta(x - \frac{k \cdot n}{p \cdot n})\delta(x_1 - \frac{k_1 \cdot n}{p \cdot n})\delta(\tilde{x}_1 - \frac{\tilde{k}_1 \cdot n}{p \cdot n})\frac{1}{2p \cdot n} \\ &\quad \int d^4y d^4y_1 d^4\tilde{y}_1 e^{-i(\tilde{k}_1 - k_1)\cdot y_1} e^{i(\tilde{k}_1 - k)\cdot \tilde{y}_1} e^{ik \cdot y} \\ &\quad \langle P_A|\bar{\psi}(0)\gamma \cdot n A_\alpha(y_1) A_\beta(\tilde{y}_1)\psi(y)|P_A\rangle, \end{aligned} \tag{3.4}$$

And the relation between $H^{\alpha\beta}_{\mu\nu}(x, \tilde{x}_1, x_1)$ and $\hat{H}^{\alpha\beta}_{\mu\nu}(x, \tilde{x}_1, x_1)$ is given by

$$H^{\alpha\beta}_{\mu\nu}(x, \tilde{x}_1, x_1, q) = \frac{1}{8\pi}\mathrm{Tr}[\gamma \cdot p \hat{H}^{\alpha\beta}_{\mu\nu}]. \tag{3.5}$$

In Eqn.(3.3), the Lorentz index α and β couple the hard part $H^{\alpha\beta}_{\mu\nu}$ with $T^{(1)}_{\alpha\beta}$. For the leading twist contribution, the Lorentz index α and β can be extracted out from $T^{(1)}_{\alpha\beta}$. Then we obtain

$$\begin{aligned} T^{(1)}_{\alpha\beta} &\simeq M_A \cdot \frac{d_{\alpha\beta}}{2} \\ M_A &= -g^{\alpha\beta} T^{(1)}_{\alpha\beta}, \end{aligned} \tag{3.6}$$

where $d^{\alpha\beta}$ is the transverse part of the gluon polarization which is defined as

$$d^{\alpha\beta} = \bar{n}^\alpha n^\beta + n^\alpha \bar{n}^\beta - g^{\alpha\beta}. \tag{3.7}$$

In Eqn.(3.4) the amplitude contains the gauge operators A_α and A_β. We can transform the gauge operators into field operators by use of the relationship between the field operator and gluon operator which is given by

$$F^a_{uv} = \partial_u A^a_v - \partial_v A^a_u + g\, f^{abc} A^b_u A^c_v. \tag{3.8}$$

Since we take the light-cone gauge $n \cdot A = 0$, after multiplied by n^μ on both sides of Eqn.(3.8), it gives

$$n^u F^a_{uv} = n^u \partial_u A^a_v. \tag{3.9}$$

Note that in Eqn.(3.9), there is the derivative on the gauge operator. We can use the partial integral to eliminate the derivative. Then we obtain

$$\begin{aligned} \int d^4y_1 e^{-iy_1\cdot(\tilde{k}_1-k_1)} n^\sigma F_{\sigma\alpha}(y_1) &= \int d^4y_1 e^{-iy_1\cdot(\tilde{k}-k_1)} n^\sigma \partial_\sigma A_\alpha(y_1) \\ &= i(\tilde{k}_1 - k_1)\cdot n \int d^4y_1 e^{-iy_1\cdot(\tilde{k}_1-k_1)} A_\alpha(y_1). \end{aligned} \tag{3.10}$$

Now we can use Eqn.(3.10) to change the gluon operators into the field operators. At the same time, we integrate out d^4k_i, dy_i^+ and $dy_i^\perp$, Eqn. (3.4) will be written as

$$\begin{aligned} T^{(1)}_{\alpha\beta} &= \int \frac{p^+ d\tilde{y}_1^-}{2\pi} \frac{p^+ dy^-}{2\pi} \frac{p^+ dy_1^-}{2\pi} \mathrm{e}^{ixp^+y^-}\, \mathrm{e}^{i(\tilde{x_1}-x)p^+\tilde{y_1}^-}\, \mathrm{e}^{-i(\tilde{x_1}-x_1)p^+y_1^-} \\ &\quad \frac{1}{2p\cdot n} \langle P_A|\bar{\psi}(0)\gamma\cdot n A_\alpha(y_1^-) A_\beta(\tilde{y}_1^-)\psi(y^-)|P_A\rangle \\ &= \frac{1}{i(\tilde{x}_1 - x_1)p^+} \cdot \frac{1}{i(x-\tilde{x}_1)p^+} \int \frac{p^+ d\tilde{y}_1^-}{2\pi} \frac{p^+ dy^-}{2\pi} \frac{p^+ dy_1^-}{2\pi} \\ &\quad \frac{1}{2p\cdot n} \mathrm{e}^{ixp^+y^-}\, \mathrm{e}^{i(\tilde{x_1}-x)p^+\tilde{y_1}^-}\, \mathrm{e}^{-i(\tilde{x_1}-x_1)p^+y_1^-} \langle P_A|\bar{\psi}(0)\gamma\cdot n F_{+\alpha}(y_1^-) F_{+\beta}(\tilde{y}_1^-)\psi(y^-)|P_A\rangle \end{aligned} \tag{3.11}$$

The last equation of Eqn.(3.11) is obtained by use of Eqn.(3.10).

Then using Eqn.(3.6), we obtain

$$\begin{aligned} M_A &= \frac{-1}{x_1 - \tilde{x_1} - i\epsilon} \frac{1}{\tilde{x_1} - x - i\epsilon} \int \frac{dy^-}{2\pi} \frac{dy_1^-}{2\pi} \frac{d\tilde{y_1}^-}{2\pi}\, \mathrm{e}^{ixp^+y^-}\, \mathrm{e}^{i(\tilde{x_1}-x)p^+\tilde{y_1}^-}\, \mathrm{e}^{-i(\tilde{x_1}-x_1)p^+y_1^-} \\ &\quad \langle P_A|\bar{\psi}(0)\frac{\gamma^+}{2} F^{+\alpha}(y_1^-) F_\alpha{}^+(\tilde{y_1}^-)\psi(y^-)|P_A\rangle\,. \end{aligned} \tag{3.12}$$

We adapt the $i\epsilon$ prescription introduced in Ref. (13) for the two poles $1/(x_1 - \tilde{x_1})$ and $1/(\tilde{x_1} - x)$.

When we plug Eqn.(3.6), Eqn.(3.11) and Eqn.(3.12) into Eqn.(3.3), the hadronic tensor $W^{(1)}_{\mu\nu}$ will be

$$W^{(1)}_{\mu\nu} = \int dx d\tilde{x}_1 dx_1 \frac{1}{2} d_{\alpha\beta} H^{\alpha\beta}_{\mu\nu}(x, \tilde{x}_1, x_1, q) M_A(x, \tilde{x}_1, x_1). \qquad (3.13)$$

Now we have obtained the general expression for hadronic tensor $W^{(1)}_{\mu\nu}$ with double scattering effect. The hadronic tensor is expressed as the convolution between hard part $H^{\alpha\beta}_{\mu\nu}$ and multiple parton correlation function M_A.

If we consider the production of a single hadron of momentum p_h in DIS, we have the non-perturbative part $D_{q\to h}(z_h)$ which represents the fragmentation function. With this fragmentation function, the hadronic tensor $W^{(1)}_{\mu\nu}$ with the double scattering effect is given by

$$\begin{aligned}\frac{dW_{\mu\nu}}{dz_h} &= \sum_q \int dz\, dz_1\, \mathcal{D}_{q\to h}(z, z_1, Q^2) \int dx\, d\tilde{x_1}\, dx_1\, \delta(z - \frac{2xp\cdot p_h}{Q^2})\, \delta(z_1 - \frac{2x_1 p\cdot p_h}{Q^2}) \\ &\times M_A(x, \tilde{x_1}, x_1)\, H^{(D)}_{\mu\nu}(x, \tilde{x_1}, x_1, x_B, z, z_1)\,. \qquad (3.14)\end{aligned}$$

If the partonic part, $H^{(D)}_{\mu\nu}(x, \tilde{x_1}, x_1, x_B, z, z_1)$, is a nonvanish smooth function at the poles, which will be verified later, the two unpinched poles in Eqn. (3.12) can be used to perform the contour integration for $d\tilde{x_1}\, dx_1$ in Eqn. (3.14). In this sense, the hadronic matrix element M_A can be effectively written as

$$M_A(x, \tilde{x_1}, x_1) \to \delta(\tilde{x_1} - x)\, \delta(x_1 - \tilde{x_1})\, \mathcal{F}_A(x, \tilde{x_1}, x_1) \qquad (3.15)$$

with the function $\mathcal{F}_A$ defined as

$$\begin{aligned}\mathcal{F}_A(x, \tilde{x_1}, x_1) &= \int \frac{dy^-}{2\pi} \frac{dy_1^-}{2\pi} \frac{d\tilde{y_1}^-}{2\pi}\, \mathrm{e}^{ixp^+y^-}\, \mathrm{e}^{i(\tilde{x_1}-x)p^+\tilde{y_1}^-}\, \mathrm{e}^{-i(\tilde{x_1}-x_1)p^+y_1^-} \\ &\times (2\pi)^2 \theta(y_1^-)\, \theta(\tilde{y_1}^-)\, \langle P_A|\bar{\psi}(0)\frac{\gamma^+}{2} F^{+\alpha}(y_1^-) F_\alpha{}^+(\tilde{y_1}^-)\psi(y^-)|P_A\rangle. \end{aligned}$$

(3.16)

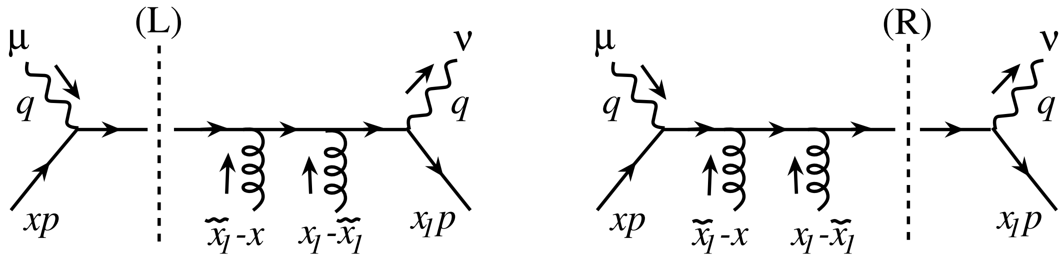

Figure 3.4 Lowest order double scattering Feynman diagrams that contribute to the hard part of the leading power $A^{1/3}$-type nuclear enhancement.

The partonic part $H^D_{\mu\nu}$ in Eqn. (3.14) is given by the Feynman diagrams in Fig. 3.4 with the quark lines contracted by $\frac{1}{2}\gamma\cdot p$ and gluon lines contracted by $\frac{1}{2}d_{\alpha\beta}$. The transverse tensor $d_{\alpha\beta} = -g_{\alpha\beta} + \bar{n}_\alpha n_\beta + n_\alpha \bar{n}_\beta$ with two lightlike vectors, $n = (n^+, n^-, n_T) = (0, 1, 0_\perp)$ and $\bar{n} = (1, 0, 0_\perp)$. The leading pole contribution of $H^D_{\mu\nu}$ with cut on the left side is

$$H^D_{\mu\nu}|_{L-cut} = e^T_{\mu\nu}\left(\frac{1}{2}e_q^2\right)\left(\frac{2\pi\alpha_s}{3}\right)\frac{1}{Q^2}x_B\frac{\delta(x-x_B)}{x_1-x}, \tag{3.17}$$

and the contribution with cut on the right side is

$$H^D_{\mu\nu}|_{R-cut} = e^T_{\mu\nu}\left(\frac{1}{2}e_q^2\right)\left(\frac{2\pi\alpha_s}{3}\right)\frac{1}{Q^2}x_B\frac{\delta(x_1-x_B)}{x-x_1}. \tag{3.18}$$

As we can see, the individual contribution of Eqn. (3.17) and Eqn. (3.18) is divergent. However, the sum of the contributions is finite.

Summing up contributions from the both cuts, and using Eqn. (3.14), Eqn. (3.17), Eqn. (3.18) and Eqn. (3.15), we have the leading order contribution from the double final state scattering:

$$\begin{aligned}\frac{dW^{(1)}_{\mu\nu}}{dz_h} &= \int dx\,dx_1\,\mathcal{F}_A(x,x,x_1)\int dz\,dz_1\,\delta(x-z\frac{Q^2}{2p\cdot p_h})\,\delta(x_1-z_1\frac{Q^2}{2p\cdot p_h})\\ &\quad \delta(z-z_1)\mathcal{D}_{q\to h}(z,z_1,Q^2)\,\frac{x_B}{Q^2}\,\frac{Q^2}{2p\cdot p_h}\left[\frac{\delta(z-z_h)}{z_1-z}+\frac{\delta(z_1-z_h)}{z-z_1}\right]\end{aligned} \tag{3.19}$$

with an overall proportional constant factor $(e^T_{\mu\nu}/2)\,e_q^2\,(2\pi\alpha_s/3)$ from the hard parts in Eqn. (3.17) and Eqn. (3.18) and a sum over all quark and antiquark flavor. Because of the $\delta(z-z_1)$, we can expand the z_1 in above expression inside the square bracket around z:

$$\frac{\delta(z-z_h)}{z_1-z}+\frac{\delta(z_1-z_h)}{z-z_1}\approx -\delta'(z-z_h)\ . \tag{3.20}$$

Combining Eqn. (3.19) and Eqn. (3.20), and carrying out all integrations by using the δ-functions, we have

$$\begin{aligned}\frac{dW^{(1)}_{\mu\nu}}{dz_h} &= \frac{1}{2}e^T_{\mu\nu}\sum_q e_q^2\left(\frac{4\pi^2\alpha_s}{3}\right)\frac{x_B}{Q^2}\frac{d}{dx_B}T^A_{qg}(x_B,Q^2)\,D_{q\to h}(z_h,Q^2)\\ &+ \frac{1}{2}e^T_{\mu\nu}\sum_q e_q^2\left(\frac{4\pi^2\alpha_s}{3}\right)\frac{z_h}{Q^2}\,T^A_{qg}(x_B,Q^2)\,\frac{dD_{q\to h}(z_h,Q^2)}{dz_h}\end{aligned} \tag{3.21}$$

where $\sum_q$ runs over all quark and antiquark flavors, and the twist-4 quark-gluon correlation function is defined as (12)

$$\begin{aligned}T^A_{qg}(x_B,Q^2) &= \int\frac{dy^-}{2\pi}\,e^{ix_Bp^+y^-}\int\frac{dy_1^-d\tilde{y}_1^-}{2\pi}\,\theta(y_1^-)\,\theta(\tilde{y}_1^-)\\ &\times\langle P_A|\bar{\psi}_q(0)\,\frac{\gamma^+}{2}\,F^{+\alpha}(y_1^-)F_\alpha{}^+(\tilde{y}_1^-)\psi_q(y^-)|P_A\rangle\ .\end{aligned} \tag{3.22}$$

This result shows that interference of amplitudes with different parton-level multiple scatterings affects the hadron production rate in semi-inclusive DIS. The effect is sensitive to the slope of incoming parton flux as well as the shape of the fragmentation function. When combined with the lowest order in Eqn. (2.36), the first term in Eqn. (3.21) is responsible for the high twist shadowing of inclusive deep inelastic scattering (DIS) (14). It will not be included in the rest discussion of the hadron production rate.

3.2 A-Enhancement Contribution

In the last section, we calculated the two Feynman diagrams which give the contribution to the hadronic tensor $W^{(1)}_{\mu\nu}$ with the double scattering effect. And we need to prove that both of them will give the $A^{1/3}$- type of nuclear size enhancement.

The partonic hard part is independent of the structure of the nuclear matter. Therefore, the only source for the nuclear size enhancement should come from the multiple parton correlation function.

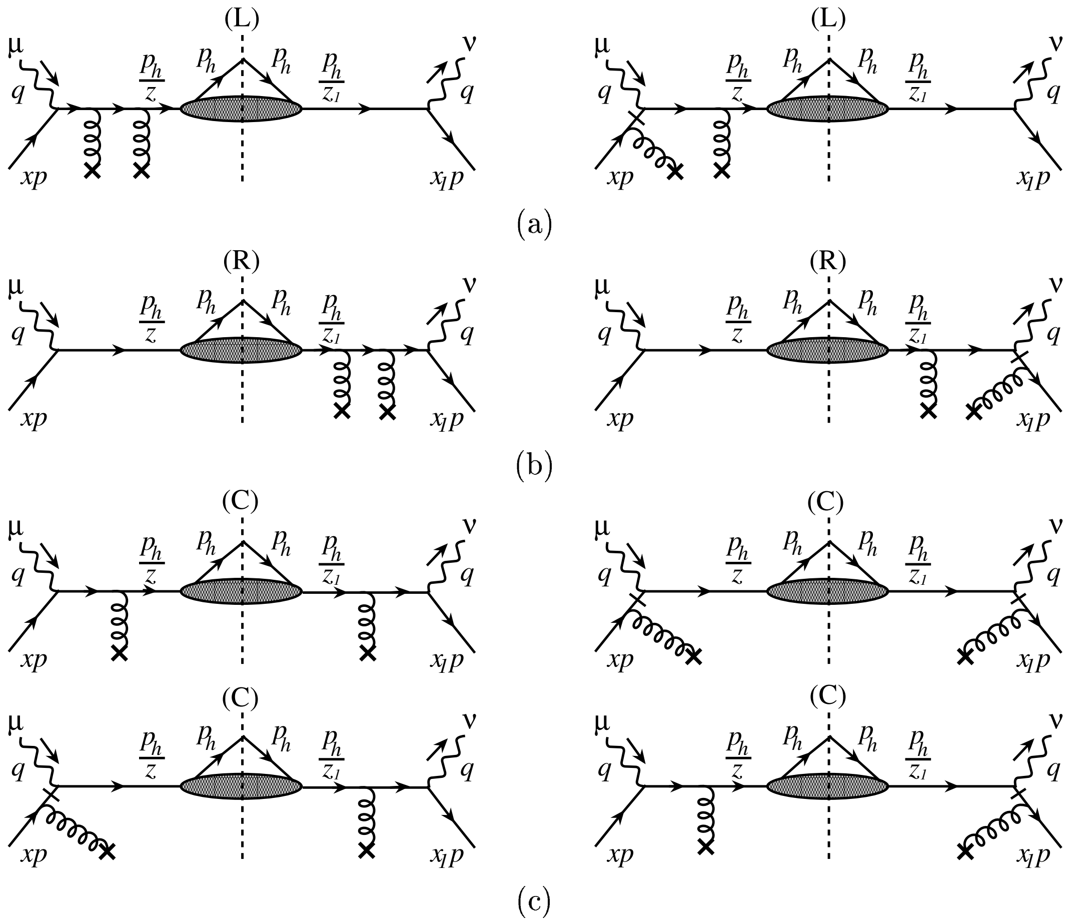

Figure 3.5 Leading order double scattering Feynman diagrams that contribute to the semi-inclusive deep inelastic scattering on a quark state. Diagrams of (a) and (b) give explicit $A^{1/3}$-type medium size enhancement; and diagrams of (c) give localized contributions.

From Eqn. (3.22), we can see that each pair of fields represents a parton that participates in the hard scattering. The y_i^- integrals parameterize the distance between the positions of these particles along the path of the outgoing scattered quark. The integrals over the distance y_i^- generally can not grow with the size of the medium because of the exponential factors $e^{iP^+\tilde{x}_i y_i^-}$ where $\tilde{x}_i$ represents the fraction of nuclear momentum carried by the gluons. If $\tilde{x}_i \sim 0$, then the corresponding y_i^- integration can be proportional to the nuclear size $A^{1/3}$.

Fig. 3.5 shows leading order double scattering Feynman diagrams for the semi-inclusive hadronic tensor on a quark state. The fermion lines with a short bar represent the contact terms quark propagators, and diagrams with both gluons attached to the incoming quark line vanish (11). Although all diagrams in Fig. 3.5 could contribute to the production rate of the hadron in semi-inclusive DIS, as we discuss below, only diagrams in Figs. 3.5(a) and (b) can give the leading power contribution in the $A^{1/3}$-type medium size enhancement. In terms of Feynman diagram, contribution of every propagator consists of two parts: a potential pole contribution and a contact contribution (11). For example, a quark propagator of momentum k can always be written as

$$\frac{i\gamma\cdot k}{k^2+i\epsilon} = \frac{i\gamma\cdot\hat{k}}{k^2+i\epsilon} + \frac{i\gamma\cdot n}{2k\cdot n}\,\frac{k^2}{k^2+i\epsilon}\ , \tag{3.23}$$

where $\hat{k}^2 = 0$ and n^μ is any auxiliary vector with $k\cdot n \neq 0$. The first term in the right-hand-side of Eqn. (3.23) corresponds the potential pole contribution when $k^2 \to 0$, while the second term is the contact contribution (11). Attaching one gluon to the initial quark line introduces a quark propagator, and this propagator will have both the pole and contact contributions. The pole contribution is long-distance in nature, representing the interactions between the quark and the gluon long before the hard collision between the quark and the virtual photon. The pole contribution of the incoming quark propagator should be a part of the nuclear quark distribution, and is partially responsible for the relatively weak A-dependence of the leading-twist parton distributions in a nucleus (15; 16). On the other hand, the contribution of the contact term is localized in space (11), and does not result into the $A^{1/3}$ type of nuclear enhancement (17). Since Feynman diagrams in Fig. 3.5(c) form a gauge invariant subset of short-distance partonic contributions, this set of diagrams will not contribute to the leading $A^{1/3}$-type of nuclear enhancement. Diagrams with the initial-state contact interactions in Figs. 3.5(a) and (b) vanish, while the other two diagrams with final-state rescattering will have at least one pole contribution.

The pole contribution from diagrams with the final-state rescattering, shown in Figs. 3.5(a) and (b), is responsible for the leading $A^{1/3}$-type of nuclear enhancement, because taking the residue of the unpinched pole effectively sets the gluon momentum to zero and leaves the corresponding coordinate space integration of the gluon field to the size of nucleus.

In the last section, we have obtained the multiple parton correlation function T_{qg}^A. We expect that this multiple parton correlation function can give the nuclear size enhancement. Since it is non-perturbative it must be taken from experiment. At the same time, we expect that the probability to detect the hard parton to be essentially unaffected by the presence of the additional soft scattering. Therefore we choose the ansatz (12)

$$T_{qg}^A(x_B, Q^2) \;=\; \lambda^2\, A^{1/3}\, \phi_q(x_B, Q^2), \tag{3.24}$$

where λ is a constant with dimension of mass and $\phi_q(x_B, Q^2)$ is the parton distribution function.

Using the ansatz Eqn.(3.24), we can get

$$\frac{dW_{\mu\nu}^{(1)}}{dz_h} = \frac{1}{2}\, e_T^{\mu\nu} \sum_q e_q^2\, (\frac{4\pi^2\alpha_s}{3})\, \frac{\lambda^2\, A^{1/3}\, z_h}{Q^2}\, \phi_q(x_B, Q^2)\, \frac{dD_{q\to h}(z_h)}{dz_h}. \tag{3.25}$$

3.3 Generalization to n-additional Scattering

In the previous section, we have seen that how the coherently double scattering affects the parton fragmentation function. Now we would generalize the double scattering into the n-additional scattering.

To compute the effect of higher order final state multiple scattering, we add pairs of gluon interactions to the struck quark and convert the gluon field operators in the hadronic matrix element of $W^{\mu\nu}$ to the corresponding field strength. Each pair of gluon interaction will contribute a factor of (14)

$$x_B \frac{2\pi\alpha_s}{3Q^2} \int \frac{dy_i^-}{2\pi}\, \frac{d\tilde{y}_i^-}{2\pi}\, \frac{e^{i(x_i-\tilde{x}_i)p^+ y_i^-}}{x_i - \tilde{x}_i - i\epsilon}\, \frac{e^{i(\tilde{x}_i - x_{i-1})p^+ \tilde{y}_i^-}}{\tilde{x}_i - x_{i-1} - i\epsilon} F^{+\alpha}(y_i^-) F_\alpha^{\ +}(\tilde{y}_i^-) \begin{cases} \frac{-1}{x_{i-1} - x_B + i\epsilon} & \text{L} \\ \frac{-1}{x_i - x_B - i\epsilon} & \text{R} \end{cases}. \tag{3.26}$$

"L" ("R") means the gluon pair are to the left (right) of the final state cut line.

To obtain the leading pole contribution for the partonic part with n additional scattering, we need to sum over all diagrams with all possible insertions of the n gluon pairs to both sides of the final state cut line. Similar to Eqn. (3.15) we can replace the poles in Eqn. (3.26) by corresponding δ- functions, expand all x_i of $\delta(x_i - x)$ around x, and obtain

$$H^n_{\mu\nu} \;=\; e^T_{\mu\nu}\left(\frac{1}{2}\,e_q^2\right)\left(\frac{2\pi\alpha_s}{3}\right)^n\left(\frac{x}{Q^2}\right)^n(-1)^n\frac{d^n}{dx}\delta(x-x_B)\,. \tag{3.27}$$

After carrying out the rest integrals by using δ-functions, we obtain the leading pole contribution for semi-inclusive hadronic tensor, with n additional scattering:

$$\frac{dW^{(n)}_{\mu\nu}}{dz_h} \simeq \frac{1}{2}\,e^T_{\mu\nu}\sum_q e_q^2\,[z_h\,\frac{4\pi^2\alpha_s}{3Q^2}]^n\,\frac{1}{n!}\,M_A^{(n)}(x_B,Q^2)\,\frac{d^n}{dz_h^n}\,D_{q\to h}(z_h,Q^2), \tag{3.28}$$

where the multiple-field operator $M_A^{(n)}(x_B,Q^2)$ is defined as

$$M_A^{(n)}(x_B,Q^2) \;=\; \int\frac{dy_0^-}{2\pi}\,e^{ixp^+y_0^-}\,\langle P_A|\bar\psi_q(0)\frac{\gamma^+}{2}\psi_q(y_0^-)\,\prod_{i=1}^n[\int p^+\,dy_i^-\theta(y_i^-)\,\hat F^2(y_i^-)]|P_A\rangle \tag{3.29}$$

The integration $\int p^+dy_i^-$ in Eqn. (3.29) gives the nuclear size dependence (16). And the operator $\hat F^2(y_i^-)$ is given by

$$\hat F^2(y_i^-) \equiv \int\frac{d\tilde y_i{}^-}{2\pi}\;\frac{F^{+\alpha}(y_i^-)F_\alpha{}^+(\tilde y_i{}^-)}{p^+}\,\theta(\tilde y_i{}^-)\;. \tag{3.30}$$

Comparing with the operator definition of gluon density, we can see that its expectation value can be related to the small-x limit of the gluon distribution, $\langle p|\hat F^2(y_i^-)|p\rangle \approx \lim_{x\to 0}\frac{1}{2}\,x\,G(x,Q^2)$, and is independent of y_i (14).

In order to evaluate the multi-field matrix element in Eqn. (3.29), we approximate the expectation value of the product of operators to be a product of expectation values of the basic operator units in a nucleon state of momentum $p = P_A/A$:

$$\langle P_A|\,\hat O_0\,\prod_{i=1}^n\hat O_i\,|P_A\rangle = A\,\langle p\,|\,\hat O_0\,|\,p\rangle\prod_{i=1}^n\left[N_p\,\langle p\,|\,\hat O_i\,|\,p\rangle\right]\;, \tag{3.31}$$

where N_p is the normalization. In a model of constant lab frame nucleus density $\rho(r) = 3/(4\pi r_0^3)$, we have

$$\int p^+ dy_i^- \theta(y_i^-) N_p \langle p|\hat{F}^2(y_i^-)|p\rangle = \frac{9}{16\pi r_0^2}(A^{1/3}-1)\langle p|\hat{F}^2(y_i^-)|p\rangle \tag{3.32}$$

The factor $(A^{1/3}-1)$ is taken such that the nuclear effect vanishes for $A=1$. With the above model for $M_A^{(n)}$, we have

$$\frac{dW_{\mu\nu}^{(n)}}{dz_h} \approx \frac{1}{2} e_{\mu\nu}^T \sum_q e_q^2 \, A \, \phi_q(x_B, Q^2) \left[\frac{z_h \, \kappa^2 (A^{1/3}-1)}{Q^2}\right]^n \frac{1}{n!} \frac{d^n}{dz_h^n} D_{q\to h}(z_h, Q^2) \tag{3.33}$$

The quantity κ^2 represent the characteristic scale of quark interaction with the medium (14)

$$\kappa^2 \;=\; \frac{3\pi\alpha_s(Q^2)}{4\, r_0^2} \langle p|\, \hat{F}^2(y_i)\, |p\rangle \; . \tag{3.34}$$

Summing the $A^{1/3}$-enhanced contributions in Eqn. (3.33) to all order in n, we have

$$\begin{aligned} \frac{dW_{\mu\nu}^{(n)}}{dz_h} \;&\simeq\; \frac{1}{2}\, e_{\mu\nu}^T \sum_q e_q^2 \, \Phi_q(x, Q^2) \sum_{n=0}^{N} \frac{1}{n!} \left[\frac{z_h \, \kappa^2 \, (A^{1/3}-1)}{Q^2}\right]^n \frac{d^n D_{q\to h}(z_h, Q^2)}{dz_h^n} \\ &\simeq\; A \, \frac{1}{2}\, e_{\mu\nu}^T \sum_q e_q^2 \, \Phi_q(x, Q^2) \, D_{q\to h}(z_h + \frac{z_h \, \kappa^2 \, (A^{1/3}-1)}{Q^2}, Q^2), \end{aligned} \tag{3.35}$$

where N is the upper limit on the number of quark-nucleon interactions. In deriving Eqn. (3.35) we have taken $N \approx \infty$ because the effective value of κ^2 is relatively small. Eqn. (3.35) is the main result of this paper. It shows that the net effect of quantum interference of amplitudes with multiple scattering of propagating quark in the medium is equivalent to a shift in the variable z_h for the quark fragmentation function $D_{q\to h}(z)$, which leads to a suppression of the hadron production rate. Such a shift in z_h for the fragmentation function is very similar to the effect of the parton energy loss model proposed in Ref. (18). The shift

$$\Delta z_h = z_h \, \frac{\kappa^2 (A^{1/3}-1)}{Q^2} \tag{3.36}$$

depends on only one parameter κ^2 and the medium length. The parameter $\kappa^2 \propto \lim_{x\to 0} xG(x, Q^2)$. It can be related to the λ^2 in LQS model for twist-4 quark-gluon correlation function $T_{qg}(x) = A^{4/3}\lambda^2\phi_q(x)$ (12) by $\kappa^2 = (4\pi^2\alpha_s/3)\lambda^2$. The λ^2 has been estimated using Drell-Yan transverse momentum broadening and DIS momentum imbalance (12; 19), and was in the range of $0.01 - 0.1$ GeV^2.

CHAPTER 4. COMPARISON WITH EXPERIMENTAL DATA

From Chapter 3, we obtain our main result Eqn.(3.35). We found that the net effect of coherent multiple scattering of a propagating quark in the medium, is equivalent to a shift Δz_h in the variable z_h of the quark fragmentation function $D_{q\to h}(z_h, Q^2)$. The shift $\Delta z_h = z_h \frac{\kappa^2 (A^{1/3}-1)}{Q^2}$. Since light quark fragmentation functions are a decreasing function of the variable z_h, the effective shift Δz_h changing z_h into larger number $z_h + \Delta z_h$ would rescale z_h and lead to a suppression of the fragmentation function compared with the fragmentation function without rescaling at each fixed point z_h. Physically, this corresponds to the suppression of hadron production.

In order to compare our result with experiment, we consider the influence of the nuclear medium on the production of the charged hadrons in semi-inclusive DIS studied by the HERMES experiment by use of 27.6 GeV positrons off deuterium, nitrogen and krypton targets. The experimental results for semi-inclusive DIS on nuclei are presented in terms of the hadron multiplicity ratio R_M, which represents the ratio of the number of hadrons produced per deep-inelastic scattering event on a nuclear target of mass A to that from a deuterium target(D). The multiplicity ratio R_M is defined as

$$R_M = \frac{N_h^A(z_h,\nu)}{N_e^A(\nu)} / \frac{N_h^D(z_h,\nu)}{N_e^D(\nu)}, \tag{4.1}$$

where $N_h(z_h,\nu)$ is the number of semi-inclusive hadrons, and $N_e(\nu)$ is the number of inclusive DIS positions.

In the QCD improved parton model, the ratio can be expressed as

$$R_M \equiv \frac{R^A}{R^D} \approx \frac{\sum_q e_q^2\, \phi_q^A(x_B,Q^2)\, D_{q\to h}^A(z_h,Q^2)}{\sum_q e_q^2\, \phi_q^D(x_B,Q^2)\, D_{q\to h}^D(z_h,Q^2)} \frac{\sum_q e_q^2\, \phi_q^D(x_B,Q^2)}{\sum_q e_q^2\, \phi_q^A(x_B,Q^2)}, \tag{4.2}$$

where A represents the nucleus and D represents the Deuterium.

If we consider the coherent multiple scattering effect, using our result Eqn.(3.35), the relation between the fragmentation function $D_{q\to h}^A(z_h,Q^2)$ and the original fragmentation function $D_{q\to h}(z_h)$ can be written as

$$D_{q\to h}^A(z_h,Q^2) \;=\; D_{q\to h}(z_h+\Delta z_h). \tag{4.3}$$

To obtain the numerical estimate of the double ratio R_M, we use the lowest order CTEQ6 parton distributions (20). For the nuclear dependence of parton distribution, we use the parameterizations given in Ref. (21). As a result, the multiplicity ratio R_M will be

$$R_M \equiv \frac{R^A}{R^D} \approx \frac{\sum_q e_q^2\, \phi_q^A(x_B,Q^2)\, D_{q\to h}(z_h+\Delta z_h,Q^2)}{\sum_q e_q^2\, \phi_q^D(x_B,Q^2)\, D_{q\to h}(z_h,Q^2)} \frac{\sum_q e_q^2\, \phi_q^D(x_B,Q^2)}{\sum_q e_q^2\, \phi_q^A(x_B,Q^2)}, \tag{4.4}$$

If we choose the krypton target with nuclear number $A = 84$, the shift Δz_h will be given for each value of z_h. The fitting results are shown in Fig.4.1 and Fig.4.2. In Fig.4.1, the final-state charged hadrons are Pions. In Fig.4.2, the final-state charged hadrons are Kaons.

In both Fig.4.1 and Fig.4.2, the dashed lines are obtained from Eqn. (4.4) and the dot-dashed lines includes only the double scattering. From the HERMES experimental data (22), we can see that the multiplicity ratio R_M is smaller than 1 for all the range of z_h. Our fitting results describe qualitatively the shape of the experimental data. However at large z_h, resumed theory curves are much steeper than the data. This more suppression can be attenuated by considering the in-medium prehadron formation. In this model, the struck parton first neutralizes its color and becomes a prehadron. Then the prehadron will collapse on the observed hadron wave function outside the nucleus. The prehadron formation time is proportional to $(1 - z_h)$ (23). So for the larger z_h, the formation time is smaller. It means that the prehadron state forms faster for the larger z_h. Therefore, the number of scattering for the propagating parton at large z_h, or the shift, should be reduced (9). Since the hadron formation time is proportional to $(1 - z_h)$ (23), we modify Δz_h by multiplying a factor $(1 - z_h)$ and produce the solid lines in Fig. 4.1 and Fig. 4.2..

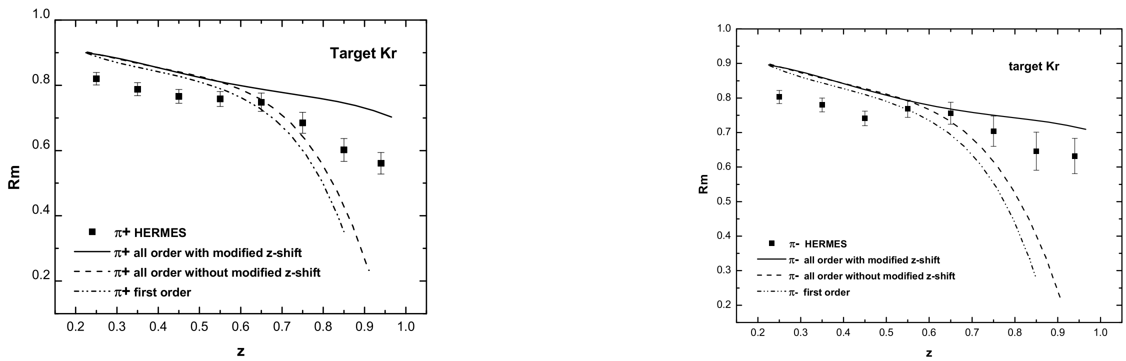

Figure 4.1 Suppression of π^+ and π^- production from multiple scattering compared with HERMES data.

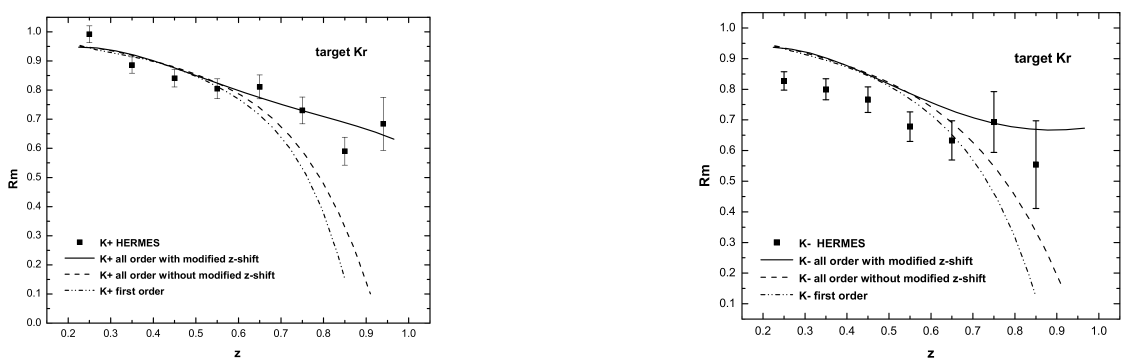

Figure 4.2 Suppression of K^+ and K^- production from multiple scattering compared with HERMES data.

As we already discussed, there are two kinds of energy loss for a propagating parton. One is the collisional energy loss. The other one is media-induced gluon radiation. Both effects have a influence on the suppression of hadron production. Therefore the suppression from the coherent multiple scattering, calculated here, complements the suppression from medium-induced radiation (8), which should give additional suppression and bring down the curves in both Fig. 4.1 and Fig. 4.2 (9).

CHAPTER 5. SUMMARY AND DISCUSSION

Using factorization, we have showed that coherent multiple scattering of a propagating parton in the nuclear medium, without the media-induced gluon radiation, can change the parton fragmentation function. The net effect of the coherent multiple scattering is equivalent to a shift from the fraction z_h of virtual photon momentum into $z_h + \Delta z_h$ in the fragmentation function. The shift Δz_h depends on the one parameter κ^2 which can be determined by the experiment.

At first we calculated the double scattering process. Then we generalized the double scattering into the n-additional scattering. We showed that even though the cross section is suppressed by the power $1/Q^2$ for each additional scattering, it can be enhanced by the nuclear size, which is proportional to $A^{1/3}$. That is why the nuclear corrections to the fragmentation function is so important that we need to sum over all order contributions to get the effective shift of the fragmentation function.

We also argue that our result requires coherence in the final state interaction between the struck parton and the nuclear medium. This is complementary to the dynamics of energy loss by the media-induced gluon radiation from the struck parton.

The comparison between our result and the experimental data is presented. Using our result, we calculated the multiplicity ratio R_M between nucleus target Krypton and Deuterium. Complementary to the effect from media-induced gluon radiation, our result can explain the suppression of hadron production by use of the prehadron formation in the semi-inclusive DIS.

Our approach can be generalized to hadron production in $p+A$ and $A+A$ collisions.

Our result can be used to understand the P_t suppression of hadron production in RHIC.

BIBLIOGRAPHY

[1] S. S. Adler *et al.* [PHENIX Collaboration], Phys. Rev. Lett. **91**, 072301 (2003); and references therein.

[2] M. Gyulassy and X. N. Wang, Nucl. Phys. B **420**, 583 (1994); X. N. Wang, M. Gyulassy and M. Plumer, Phys. Rev. D **51**, 3436 (1995); R. Baier, Y. L. Dokshitzer, A. H. Mueller, S. Peigne and D. Schiff, Nucl. Phys. B **484**, 265 (1997); B. G. Zakharov, JETP Lett. **63**, 952 (1996); JETP Lett. **65**, 615 (1997); U. A. Wiedemann, Nucl. Phys. B **588**, 303 (2000).

[3] Y. L. Dokshitzer and D. E. Kharzeev, Phys. Lett. B **519**, 199 (2001).

[4] S. S. Adler *et al.* [PHENIX Collaboration], Phys. Rev. Lett. **96**, 032301 (2006); J. Bielcik [STAR Collaboration], Nucl. Phys. A **774**, 697 (2006).

[5] J. W. Qiu and G. Sterman, Int. J. Mod. Phys. E **12**, 149 (2003).

[6] J. Aubert *et al.* [EMC Collaboration], Phys. Lett. **123**, 275 (1983).

[7] J. W. Cronin *et al.*, Phys. Rev. D **11**, 3105 (1975).

[8] X. F. Guo and X. N. Wang, Phys. Rev. Lett. **85**, 3591 (2000); X. N. Wang and X. F. Guo, Nucl. Phys. A **696**, 788 (2001); E. Wang and X. N. Wang, Phys. Rev. Lett. **89**, 162301 (2002).

[9] M. H. Thomas, Phys. Lett. B **273**, 128 (1991); E. Braaten and M. H. Thoma, Phys. Rev. D **44**, 2625 (1991); P. Romatschke and M. Strickland, Phys. Rev. D **71**, 125008 (2005).

[10] V. N. Gribov and L. N. Lipatov, Yad. Fiz. **15**, 781 (1972); G. Altarelli and G. Parisi, Nucl. Phys. B**126**, 298 (1977); Y. L. Dokshitzer, Sov. Phys. JETP **46**, 641 (1977).

[11] J. W. Qiu, Phys. Rev. D **42**, 30 (1990).

[12] M. Luo, J. W. Qiu and G. Sterman, Phys. Rev. D**49**, 4493 (1994).

[13] A. H. Mueller and J. W. Qiu, Nucl. Phys. B**268**, 427 (1986).

[14] J. W. Qiu and I. Vitev, Phys. Rev. Lett. **93**, 262301 (2004).

[15] For example, see F. E. Close, J. W. Qiu and D. G. Roberts, Phys. Rev. D**40**, 2820 (1989).

[16] J. W. Qiu, Nucl. Phys. A **715**, 309 (2003).

[17] J. W. Qiu and G. Sterman, Nucl. Phys. **B353**, 105 (1991); **B353**, 137 (1991).

[18] X. N. Wang and Z. Huang, Phys. Rev. C **55**, 3047 (1997); X. N. Wang, Z. Huang and I. Sarcevic, Phys. Rev. Lett. **77**, 231 (1996).

[19] X. F. Guo, Phys. Rev. D**58**, 114033 (1998).

[20] J. Pumplin, D. R. Stump, J. Huston, H. L. Lai, P. Nadolsky and W. K. Tung, JHEP **0207**, 012 (2002).

[21] K. J. Eskola, V .J .Kolhinen, and C .A .Salgado Eur. Phys. J. **C9**, 61 (1999). K. J. Eskola, V. J. Kolhinen, and P. V. Ruuskanen, Nucl. Phys. **B535**, 351 (1998).

[22] A. Airapetian *et al.* [HERMES Collaboration], Eur. Phys. J. C **20**, 479 (2001).

[23] A. Accardi, Nucl. Phys. A**783**, 561 (2007).